Contemporary Mathematics
Volume **586**, 2013
http://dx.doi.org/10.1090/conm/586/11668

The central-upwind finite-volume method for atmospheric numerical modeling

Ramachandran D. Nair and Kiran K. Katta

Abstract. A semi-discretized central-upwind finite-volume (CFV) scheme has been developed for atmospheric modeling applications. The non-oscillatory property of the scheme is achieved by employing high-order weighted essentially non-oscillatory (WENO) reconstruction method, and time integration relies on explicit Runge-Kutta method. The WENO reconstruction is fifth-order accurate and implemented in a dimension-split manner, and a fully 2D fourth-order reconstruction is also considered for comparison. The CFV scheme is computationally efficient and employs a compact non-staggered computational stencil with an optional positivity-preserving filter. The scheme has been validated for benchmark advection tests on the cubed-sphere. A global shallow-water model and a 2D non-hydrostatic Euler solver are also developed based on the same central finite-volume scheme.

1. Introduction

Finite-volume (FV) discretization has become a method of choice for many new generation atmospheric models, due to its inherent conservation properties and geometric flexibility to adapt various grid structures. A large class of FV methods for solving hyperbolic conservation laws are based on high-order extensions of the Godunov scheme [**G**], collectively known as the Godunov-type schemes. The central-upwind finite-volume (CFV) schemes [**KNP**, **KL**] are a subset of Godunov-type methods for solving hyperbolic conservation laws, and which combines the nice features of the classical upwind and central FV [**NT**] methods. In contrast with the upwind methods, the CFV schemes do not require characteristic decomposition of the hyperbolic system or expensive Riemann solvers. Semi-discrete formulation of CFV schemes avoid staggered grids and are relatively easy to implement, for practical applications. Our focus is on the application of CFV scheme for solving three major building blocks of a complex 3D atmospheric model: global linear transport equation with positivity preservation, shallow-water equations on the sphere which mimics the horizontal aspect of atmospheric dynamics, and the compressible 2D Euler equations in x-z plane for the vertical dynamics.

1991 *Mathematics Subject Classification.* Primary 86A10, 86-08; Secondary 76U99.

Key words and phrases. Central-upwind, finite-volume, shallow-water model, cubed-sphere, WENO method, non-hydrostatic Euler solver.

The first author was supported in part by DOE BER Program #DE-SC0001658. The National Center for Atmospheric Research is sponsored by NSF.

2. Semi-Discrete CFV Schemes

In order to describe the 2D CFV scheme, we first consider the following conservation law on (x, y) Cartesian plane with a source term S, as follows:

$$\frac{\partial U}{\partial t} + \nabla \cdot \mathbf{F}(U) = S(U) \text{ in } D \times (0, T], \tag{2.1}$$

where $U = U(x, y, t)$ is a conservative quantity with initial value $U_0 = U(x, y, 0)$, $\mathbf{F}(U)$ is a generic the flux function. The domain D is assumed to be rectangular and doubly periodic with non-overlapping rectangular cells $I_{ij} = [x_{i-1/2}, x_{i+1/2}] \otimes [y_{i-1/2}, y_{i+1/2}]$, with the grid-spacings Δx and Δy. Following [**KNP**, **KY**], the semi-discrete form on a rectangular cell I_{ij} with boundary Γ_k can be written as follows:

$$\frac{d\bar{U}_{ij}}{dt} = \frac{-1}{\Delta x \Delta y}\left[\sum_{k=1}^{4} \int_{\Gamma_k} \hat{\mathbf{F}} \cdot \mathbf{n}\right] + \bar{S}_{ij} \tag{2.2}$$

where $\bar{S}_{ij}$ is the the cell-averaged source term and, $\bar{U}_{ij}$ is the cell average which evolves in time and is subject to the following conservation constraint,

$$\bar{U}_{ij} = \frac{1}{\Delta x\, \Delta y} \int_{y_{j-1/2}}^{y_{j+1/2}} \int_{x_{i-1/2}}^{x_{i+1/2}} P_{ij}(x, y)\, dxdy. \tag{2.3}$$

In (2.3), $P_{ij}(x, y)$ is the piecewise polynomial function on I_{ij}, which is approximated by a suitable reconstruction function of targeted order of accuracy. We consider a fifth-order Weighted Essentially Non-Oscillatory (WENO5) 1D reconstruction [**BL**] with a dimension-split approach, and a fully 2D fourth-order reconstruction [**KY**]. For CFV with WENO5 reconstruction one flux-point on each cell walls are used (Fig. 1 left panel), resulting a simple FV discretization. However, with a fully 2D reconstruction each cell wall requires three flux evaluation (Fig. 1, right panel). For example, the flux integral in (2.2) on the east wall Γ_E for the fully 2D reconstruction is approximated by the Simpson's rule,

$$\int_{\Gamma_E} \hat{\mathbf{F}} \cdot \mathbf{n} \approx \frac{\Delta y}{6}\left[\hat{F}_{i+1/2,j-1/2} + 4\hat{F}_{i+1/2,j} + \hat{F}_{i+1/2,j+1/2}\right],$$

where $\hat{F}_{i+1/2,:}$ is the one-sided central-upwind flux formula [**KY**] which is dependent on the local speed $\alpha_{i+1/2,:}$ as follows (for convenience dependence on j is suppressed):

$$\hat{F}_{i+1/2} = \frac{\alpha^+_{i+1/2} F(U^-_{i+1/2}) - \alpha^-_{i+1/2} F(U^+_{i+1/2})}{\alpha^+_{i+1/2} - \alpha^-_{i+1/2}} + \frac{\alpha^+_{i+1/2}\alpha^-_{i+1/2}}{\alpha^+_{i+1/2} - \alpha^-_{i+1/2}}\left[U^+_{i+1/2} - U^-_{i+1/2}\right]$$

The local speed is given by the eigenvalues λ_ℓ of the flux Jacobian at the left ($^-$) and right ($^+$) sides of the cell interface such that

$$\alpha^+_{i+1/2} = \max\left[\lambda_\ell\left(\frac{\partial F}{\partial U}\right), 0\right], \quad \alpha^-_{i+1/2} = \min\left|\lambda_\ell\left(\frac{\partial F}{\partial U}\right), 0\right|$$

The final form of the semi-discrete CFV scheme reduces to the following ODE:

$$\frac{d\bar{U}_{ij}}{dt} = L(\bar{U}_{ij}), \tag{2.4}$$

which can be solved using a high-order explicit strong stability-preserving Runge-Kutta method [**GS**, **KNK**].

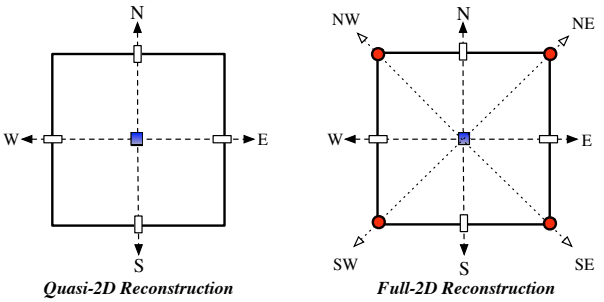

FIGURE 1. Schematic of reconstruction on CFV cells, where marked points on the cell walls denote the flux points on which fluxes are evaluated. The left panel shows a cell requiring two 1D reconstruction (WENO5) in each coordinate direction. The right panel shows a cell requiring fully 2D reconstruction for which 3 flux points on each wall.

3. The shallow water model on the cubed-sphere

The physical domain is a sphere $\mathcal{S}$, based on the cubed-sphere geometry [**SA**]. The cubed-sphere geometry consists of partitioning $\mathcal{S}$ into six identical regions which are obtained by the equiangular central projection (gnomonic) projection [**N**] of the faces of the inscribed cube onto the surface of $\mathcal{S}$. Each of the local coordinate systems is free of singularities, and creates a non-orthogonal curvilinear coordinate system on $\mathcal{S}$. However, the edges of the cubed-sphere faces are not continuous. The local coordinates (or central angles of the projection) for each face are $x^1 = x^1(\lambda,\theta)$, $x^2 = x^2(\lambda,\theta)$ such that $x^1, x^2 \in [-\pi/4, \pi/4]$, where λ and θ are the longitude and latitude, respectively, of a sphere with radius R. The metric tensor, G_{ij} associated with the transformation is

$$G_{ij} = \frac{R^2}{\rho^4 \cos^2 x^1 \cos^2 x^2} \begin{bmatrix} 1+\tan^2 x^1 & -\tan x^1 \tan x^2 \\ -\tan x^1 \tan x^2 & 1+\tan^2 x^2 \end{bmatrix},$$

where $i, j \in \{1,2\}$ and $\rho^2 = 1 + \tan^2 x^1 + \tan^2 x^2$. The Jacobian of the transformation (the metric term) is $\sqrt{G} = [\det(G_{ij})]^{1/2}$.

The flux-form shallow water (SW) model developed on the cubed-sphere relies on non-orthogonal curvilinear coordinates [**SA**]. The SW equations are treated in tensorial form with covariant (u_i) and contravariant (u^i) wind vectors, which are related through $u_i = G_{ij}u^j$, $u^i = G^{ij}u_j$ and $G^{ij} = G_{ij}^{-1}$; where $i, j \in \{1,2\}$. The orthogonal components of the spherical wind vector $\mathbf{v}(\lambda,\theta) = (u, v)$ can be expressed in terms of contravariant vectors (u^1, u^2) as follows,

$$\begin{bmatrix} u \\ v \end{bmatrix} = A \begin{bmatrix} u^1 \\ u^2 \end{bmatrix}, \quad A^T A = G_{ij}.$$

The details of the local transformation laws and A for each face of the cubed-sphere can be found in [**N**].

The governing equations for inviscid shallow-water flow (on a rotating sphere) of a thin layer of fluid (2D) are the horizontal momentum and the continuity equations for the height h. Here, h is the depth of the fluid and it is related to the free surface geopotential height (above sea level) $\Phi = g\,(h_s + h)$, where h_s denotes the height

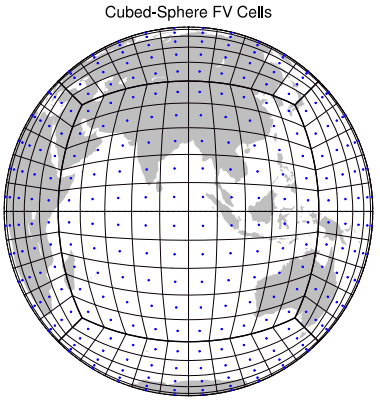

FIGURE 2. A cubed-sphere with $10 \times 10 \times 6$ FV cells (volumes), which span the entire surface of the sphere $\mathcal{S}$. On the computational domain the grid cells are uniformly spaced ($\Delta x^1 = \Delta x^2$). The halo regions required for CFV stencil at the cubed-sphere face edges are created with 1D interpolation along the grid lines.

of the underlying mountains and g is the gravitational acceleration. Thus the prognostic variables are u_1, u_2 and h, and the shallow-water equations on $\mathcal{S}$ can be written in a compact form following the formulation [**NTL**]:

$$\frac{\partial}{\partial t}\mathbf{U} + \frac{\partial}{\partial x^1}\mathbf{F}_1(\mathbf{U}) + \frac{\partial}{\partial x^2}\mathbf{F}_2(\mathbf{U}) = \mathbf{S}(\mathbf{U}), \tag{3.1}$$

where the state vector $\mathbf{U}$ and the flux vectors $\mathbf{F}_1, \mathbf{F}_2$ are defined by

$$\mathbf{U} = \left[u_1, u_2, \sqrt{G}\,h\right]^T, \quad \mathbf{F}_1 = \left[E, 0, \sqrt{G}hu^1\right]^T, \quad \mathbf{F}_2 = \left[0, E, \sqrt{G}hu^2\right]^T,$$

$E = \Phi + \frac{1}{2}\left(u_1\, u^1 + u_2\, u^2\right)$ is the energy term. The source terms $\mathbf{S}$ is a function of relative vorticity ζ, Coriolis term $f = 2\omega \sin\theta$, and the contravariant wind vectors (u^1, u^2), defined as:

$$\mathbf{S}(\mathbf{U}) = \left[\sqrt{G}u^2(f+\zeta), -\sqrt{G}\,u^1(f+\zeta), 0\right]^T, \qquad \zeta = \frac{1}{\sqrt{G}}\left[\frac{\partial u_2}{\partial x^1} - \frac{\partial u_1}{\partial x^2}\right] \tag{3.2}$$

3.1. Numerical Experiments.

3.1.1. *Conservative transport on the cubed-sphere.* The transport problem has fundamental importance for atmospheric modeling. Therefore the first test we consider is a linear transport problem, a solid-body rotation of cosine profile (cosine-bell) on the sphere, which is a benchmark test suggested in [**W**]. The transport equation on the cubed-sphere for a scalar h can be written as [**N**]:

$$\frac{\partial \psi}{\partial t} + \frac{\partial u^1 \psi}{\partial x^1} + \frac{\partial u^2 \psi}{\partial x^2} = 0, \tag{3.3}$$

where $\psi = \sqrt{G}\,h$. Note that Eq.(3.3) may be considered as a special case of (3.1) with the prescribed velocity fields.

The non-divergent velocity filed is defined to be $u = u_0(\cos\theta + \sin\lambda \sin\theta)/\sqrt{2}$, $v = -(u_0 \sin\lambda)/\sqrt{2}$. The parameter $u_0 = 2\pi R/(12 \text{ days})$, for a sphere with radius R, scaled in such a way that the wind field translates the initial cosine-bell in the

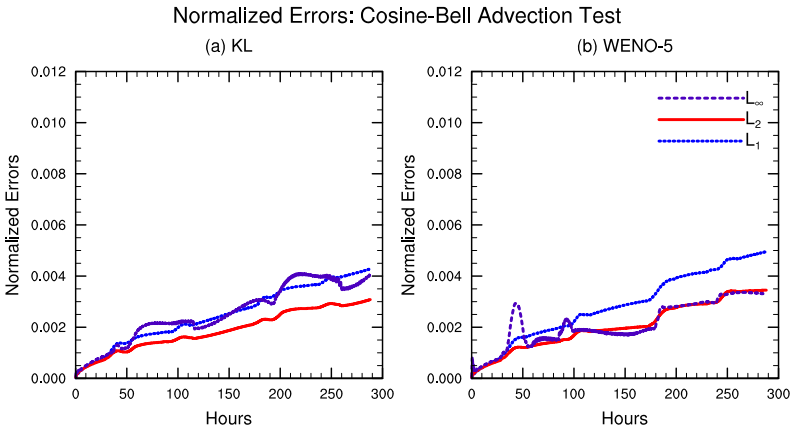

FIGURE 3. Time traces of normalized l_1, l_2, l_∞ errors for the solid-body rotation on the sphere for a complete revolution (12 days).

north-east direction, with a period of 12 days for a complete revolution. Since the exact solution is known, time tracers of the error measures (l_1, l_2, l_∞) can be computed. Initially the cosine-bell $h(\lambda, \theta, t)$ is centered at $(\lambda = 3\pi/2, \theta = 0)$ with a base radius $r_0 = R/3$

$$h(\lambda, \theta, t = 0) = \begin{cases} 500\,[1 + \cos(\pi r_d / r_0)] & \text{if } r_d < r_0 \\ 0 & \text{if } r_d \geq r_0 \end{cases},$$

where r_d is the great-circle distance between (λ, θ) and the centre of the cosine-bell.

The CFV schemes employing a fully 2D fourth-order reconstruction and a dimension split fifth-order Weighted Essentially Non-Oscillatory (WENO5) reconstruction methods are used for the transport equation (3.3). The height of the cosine-bell upon initialization is $h \in [984.2, 0]$, after a full revolution with the positivity-preserving filter [**KNK**] the height $h \in [978.6, 0]$. The resolution is $45 \times 45 \times 6$ ($\approx 2^\circ$) with CFL 0.25. Figure 3 shows the time evolution of l_1, l_2 and l_∞ errors. The fourth-order scheme scores slightly better than the split WENO5 in terms of accuracy. However, as far as the computational efficiency and ease of implementation on the cubed-sphere are concerned, the WENO5 turned out to be a better option. Hereafter, for the numerical experiments, we only report the results with the CFV scheme employing WENO5 reconstruction.

3.1.2. *Zonal flow over an isolated mountain.* This test case is particularly useful for studying the effectiveness of the numerical scheme in conserving integral invariants such as mass and total energy. For this benchmark test, the flow filed is highly nonlinear and no analytic solution is available, a complete description of this test is given in [**W**]. The initial velocity $(u, v) = (u_0 \cos\theta, 0)$ and height field is given by $g\,h = g\,h_0 - \frac{u_0}{2}(2\,a\,\omega + u_0)\sin^2\theta$, where R and ω are the earth's radius and angular velocity, respectively; $u_0 = 2\pi R/(12 \text{ days})$, and $gh_0 = 2.94 \times 10^4$ m^2/s^2. The *mountain* (circular cone) is centered at $(\lambda_c = 3\pi/2, \theta_c = \pi/6)$ with height $h_s = 2000\,(1 - r/a)$ m, where $a = \pi/9$ and $r^2 = \min[a^2, (\lambda - \lambda_c)^2 + (\theta - \theta_c)^2]$. The mean equivalent depth of the atmosphere is set to be $h_0 = 5960$ m. Figure 4 shows simulated results (WENO5) after 2 and 15 days, where an approximate resolution of 2°, and CFL ≈ 0.5 were used.

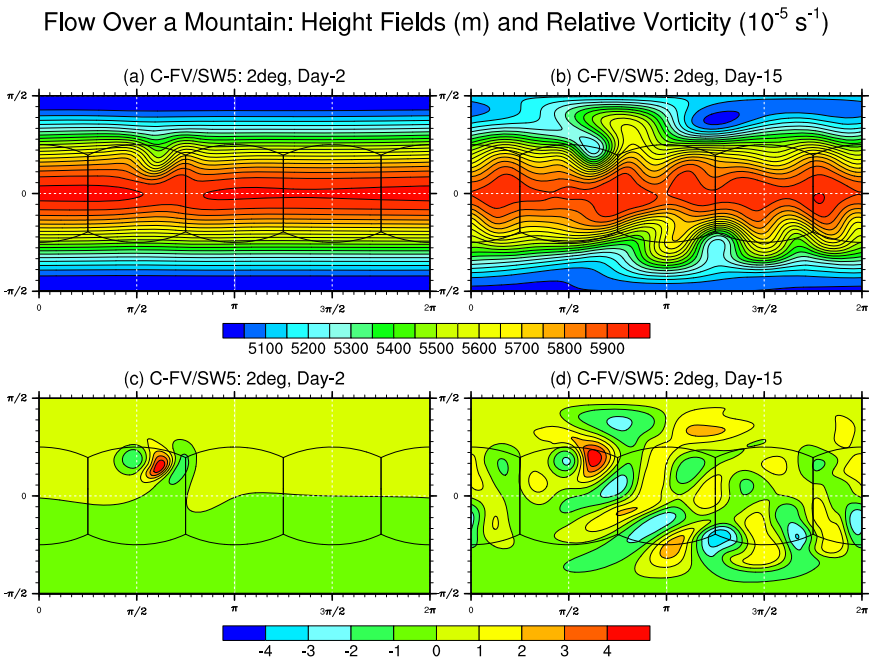

FIGURE 4. Height (top) and vorticity (bottom) fields after 2 and 15 days.

4. CFV Non-Hydrostatic 2D Model

Here we demonstrate the application of CFV for a non-hydrostatic (NH) atmospheric model, in a simple 2D (x-z) Cartesian setup. We have developed a compressible Euler solver based on CFV, which employs the following atmospheric adaptation of compressible Euler system [**GR**, **NN**]

$$\frac{\partial}{\partial t}\mathbf{U} + \frac{\partial}{\partial x}\mathbf{F}(\mathbf{U}) + \frac{\partial}{\partial z}\mathbf{G}(\mathbf{U}) = \mathbf{S}(\mathbf{U}) \tag{4.1}$$

where

$$\mathbf{U} = \begin{bmatrix} \rho' \\ \rho u \\ \rho w \\ \rho\Theta' \end{bmatrix}, \quad \mathbf{F} = \begin{bmatrix} \rho u \\ \rho u^2 + p' \\ \rho uw \\ \rho u\Theta \end{bmatrix}, \quad \mathbf{G} = \begin{bmatrix} \rho w \\ \rho wu \\ \rho w^2 + p' \\ \rho w\Theta \end{bmatrix}, \quad \mathbf{S} = \begin{bmatrix} 0 \\ 0 \\ -\rho' g \\ 0 \end{bmatrix}.$$

In the above system, ρ is the density of fluid, u is the velocity component in the x-direction (horizontal), w is the velocity component in the z-direction (vertical), p is the pressure, Θ is the potential temperature and $\mathbf{S}$ is the source term. The variables ρ, Θ and p are decomposed as the sum of mean state $(\bar{.})$ and perturbation $(.)'$; $\rho = \bar{\rho} + \rho'$, $p = \bar{p} + p'$ and $\Theta = \bar{\Theta} + \Theta'$, such that the mean-state holds hydrostatic relation $d\bar{\rho}/dz = -\bar{\rho}g$.

The potential temperature Θ and the real temperature T follow the Exner relation $\Theta = T(p_0/p)^{R_d/c_p}$. The system (4.1) is closed by the equation of state, $p = C_0(\rho\Theta)^\gamma$ where $C_0 = R_d^\gamma p_0^{-R_d/c_v}$. The reference surface pressure $p_0 = 10^5$ Pa and the other thermodynamic constants are: $\gamma = c_p/c_v$, R_d =287 J kg^{-1} K^{-1}, c_p = 1004 J kg^{-1} K^{-1}, c_v = 717 J kg^{-1} K^{-1}.

Figure 4 shows a rising bubble [**WS**, **NN**] in a convectively neutral atmosphere simulated with the CFV scheme with WENO5 reconstruction procedure. The convective thermal uses a hydrostatic balance based on a constant potential temperature with zero initial wind, and the bubble is *triggered* by perturbing the potential temperature. The model domain is $[0, 20]$ km $\times[0, 10]$ km, and grid-spacing is uniformly set to $\Delta x = \Delta z = 133$ m such that CFL ≈ 0.65, with an explicit third-order Ruge-Kutta integrator [**GS**]. Top panels in Fig. 4 shows the initial and final (1000s) thermal bubble (Θ'), and lower panels show the horizontal and vertical wind fields. The CFV Euler solver simulates bubble structure quite well as compared to other high-order model results [**WS**, **NN**].

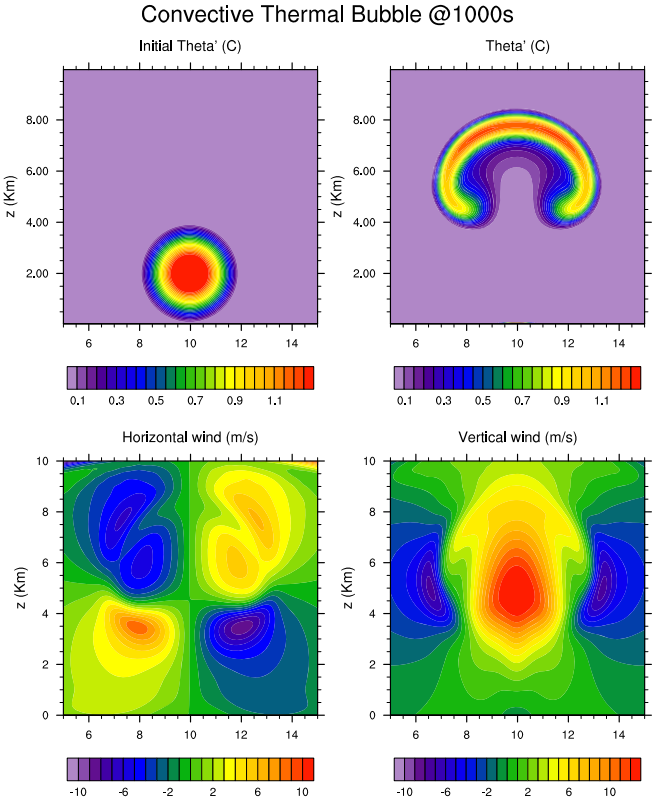

FIGURE 5. Convection in a neutral atmosphere simulated by the CFV Euler solver. Initial potential temperature perturbation (Θ') is shown in the top left panel and top right panel shows the convective bubble after 1000 s of simulation, lower left and right panels show the wind fields u and w at 1000 s, respectively.

5. Summary

We have developed a central-upwind finite volume (CFV) scheme for atmospheric modeling applications. A novel feature of this method is its simplicity, in terms of implementation. The CFV approach does not rely on characteristic

decomposition or expensive Riemann solver. The CFV scheme combined with the fifth-order WENO reconstruction employed in a dimension-split manner. The high-order dimension-split approach on the cubed-sphere did not create any significant accuracy issue as compared to a fourth-order fully 2D reconstruction. The tracer transport with CFV has the positivity-preserving option. The nonlinear shallow-water results are comparable to those with high-order conventional upwind based Godunov-type FV schemes [**CX**, **UJ**]. The Euler solver based on CFV results are promising. The 2D CFV schemes considered herein will be further extended to a 3D non-hydrostatic atmospheric model in future.

References

[BL] Steve Bryson and Doron Levy, *On the total variation of high-order semi-discrete central schemes for conservation laws*, J. Sci. Comput. **27** (2006), no. 1-3, 163–175, DOI 10.1007/s10915-005-9046-8. MR2285773 (2008c:65197)

[CX] Chungang Chen and Feng Xiao, *Shallow water model on cubed-sphere by multi-moment finite volume method*, J. Comput. Phys. **227** (2008), no. 10, 5019–5044, DOI 10.1016/j.jcp.2008.01.033. MR2414846 (2009e:86001)

[GR] F. X. Giraldo and M. Restelli, *A study of spectral element and discontinuous Galerkin methods for the Navier-Stokes equations in nonhydrostatic mesoscale atmospheric modeling: equation sets and test cases*, J. Comput. Phys. **227** (2008), no. 8, 3849–3877, DOI 10.1016/j.jcp.2007.12.009. MR2403870 (2009c:86009)

[GS] Sigal Gottlieb, Chi-Wang Shu, and Eitan Tadmor, *Strong stability-preserving high-order time discretization methods*, SIAM Rev. **43** (2001), no. 1, 89–112 (electronic), DOI 10.1137/S003614450036757X. MR1854647 (2002f:65132)

[G] S. K. Godunov, *A difference method for numerical calculation of discontinuous solutions of the equations of hydrodynamics*, Mat. Sb. (N.S.) **47 (89)** (1959), 271–306 (Russian). MR0119433 (22 #10194)

[KNK] K. Katta, R. D. Nair, and V. Kumar, *High-order central finite-volume schemes for linear transport problems on the cubed-sphere*, Quart. J. Roy. Meteor. Soc., 2012, Submitted.

[KNP] Alexander Kurganov, Sebastian Noelle, and Guergana Petrova, *Semidiscrete central-upwind schemes for hyperbolic conservation laws and Hamilton-Jacobi equations*, SIAM J. Sci. Comput. **23** (2001), no. 3, 707–740 (electronic), DOI 10.1137/S1064827500373413. MR1860961 (2003a:65065)

[KL] Alexander Kurganov and Doron Levy, *Central-upwind schemes for the Saint-Venant system*, M2AN Math. Model. Numer. Anal. **36** (2002), no. 3, 397–425, DOI 10.1051/m2an:2002019. MR1918938 (2003d:76115)

[KY] A. Kurganov and Y. Liu, *New adaptive artificial viscosity method for hyperbolic systems of conservation laws*, J. of Comput. Phys, 2012, submitted.

[N] R. D. Nair, S. J. Thomas, and R. D. Loft, *A discontinuous Galerkin transport scheme on the cubed-sphere,* Mon. Wea. Rev., **133**, 2005, pp. 814–828.

[NTL] R. D. Nair, S. J. Thomas, and R. D. Loft, *A discontinuous Galerkin global shallow water model*, Mon. Wea. Rev., **133**, pp. 876–888.

[NN] Matthew R. Norman, Ramachandran D. Nair, and Fredrick H. M. Semazzi, *A low communication and large time step explicit finite-volume solver for non-hydrostatic atmospheric dynamics*, J. Comput. Phys. **230** (2011), no. 4, 1567–1584, DOI 10.1016/j.jcp.2010.11.022. MR2753379 (2012c:86008)

[NT] Haim Nessyahu and Eitan Tadmor, *Nonoscillatory central differencing for hyperbolic conservation laws*, J. Comput. Phys. **87** (1990), no. 2, 408–463, DOI 10.1016/0021-9991(90)90260-8. MR1047564 (91i:65157)

[SA] R. Sadourny, *Conservative finite-difference approximations of the primitive equations on quasi-uniform spherical grids*, Mon. Wea. Rev., **100**, 1972, pp. 136–144.

[UJ] Paul A. Ullrich, Christiane Jablonowski, and Bram van Leer, *High-order finite-volume methods for the shallow-water equations on the sphere*, J. Comput. Phys. **229** (2010), no. 17, 6104–6134, DOI 10.1016/j.jcp.2010.04.044. MR2657861 (2011d:76069)

[W] David L. Williamson, John B. Drake, James J. Hack, Rüdiger Jakob, and Paul N. Swarztrauber, *A standard test set for numerical approximations to the shallow water equations in spherical geometry*, J. Comput. Phys. **102** (1992), no. 1, 211–224, DOI 10.1016/S0021-9991(05)80016-6. MR1177513 (93d:86006)

[WS] L. J. Wicker and W. C. Skamarock, *A time-splitting scheme for the elastic equations incorporating second-order Runge-Kutta time differencing* Mon. Wea. Rev., **126**, pp. 1992–1999

Institute for Mathematics Applied to Geosciences, National Center for Atmospheric Research, 1850 Table Mesa Drive, Boulder, Colorado 80305
E-mail address: rnair@ucar.edu

The University of Texas at El Paso, 500 W University Avenue, El Paso, Texas 79902
E-mail address: kkkatta@miners.utep.edu